

論文 / 著書情報
Article / Book Information

Title	Modular Array Structures for Design and Multiplierless Realization of Two-Dimensional Linear Phase FIR Digital Filters
Authors	Saed Samadi, AKINORI NISHIHARA, NOBUO FUJII
出典 / Citation	IEICE Tans. Fundamentals., Vol. E80-A, No. 4, pp. 722-736
発行日 / Pub. date	1997,
URL	http://search.ieice.org/
権利情報 / Copyright	本著作物の著作権は電子情報通信学会に帰属します。 Copyright (c) 1997 Institute of Electronics, Information and Communication Engineers.

PAPER

Modular Array Structures for Design and Multiplierless Realization of Two-Dimensional Linear Phase FIR Digital Filters

Saed SAMADI[†], Akinori NISHIHARA^{††}, and Nobuo FUJII^{†††}, *Members*

SUMMARY It is shown that two-dimensional linear phase FIR digital filters with various shapes of frequency response can be designed and realized as modular array structures free of multiplier coefficients. The design can be performed by judicious selection of two low order linear phase transfer functions to be used at each module as kernel filters. Regular interconnection of the modules in L rows and K columns conditioned with boundary coefficients 1, 0 and $1/2$ results in higher order digital filters. The kernels should be chosen appropriately to, first, generate the desired shape of frequency response characteristic and, second, lend themselves to multiplierless realization. When these two requirements are satisfied, the frequency response can be refined to possess narrower transition bands by adding additional rows and columns. General properties of the frequency response of the array are investigated resulting in Theorems that serve as valuable tools towards appropriate selection of the kernels. Several design examples are given. The array structures enjoy several favorable features. Specifically, regularity and lack of multiplier coefficients makes it suitable for high-speed systolic VLSI implementation. Computational complexity of the structure is also studied.

Key words: multi-dimensional filters, FIR digital filters, parallel structures, multiplierless structures, systolic arrays

1. Introduction

Design of two-dimensional (2-D) FIR digital filters has been mainly performed by windowing [1], [2] frequency sampling [3], solution of optimization problems [4]–[6], or McClellan transform methods [7], [8]. In this paper, we intend to introduce a new method for design and realization of 2-D FIR linear phase digital filters that is based on a class of modular array structures, initially proposed for one-dimensional (1-D) FIR digital filters by the authors [10]–[16]. These arrays were initially proposed for multiplierless realization of maximally flat lowpass and highpass digital filters [10], [13], [15] and then extended to maximally flat multiband filters and filters possessing ripples in their passbands and stopbands [12], [14]–[16]. These are modular structures with local connection between

neighboring modules and thus lend themselves to VLSI systolic implementation. An attractive feature of these arrays is their tolerance to the destruction of the consisting modules, a fact, established rigorously for the maximally flat lowpass case, that can be utilized for achieving graceful degradation in case of module failure [18]. Besides this interesting feature, it is also possible to obtain all possible combinations of degrees of flatness simultaneously and in an economical manner for maximally flat filters [11].

Generalization of this class of array structures to multiplierless realization of 2-D digital filters with various magnitude response shapes is not straight-forward. The main reason behind this is that for the 1-D case we have the Bernstein approximation [19], [20] and representation [21] of the linear phase frequency response as a design tool and the De Casteljau algorithm [22] as a realization tool. Generalization of the Bernstein representation to 2-D case is possible. A successful attempt to utilize the 2-D generalization of Bernstein approximation and representation to multiplierless design of 2-D digital filters can be found in [17]. In [17], a simple design method is presented as a closed-form formula for the transfer function of diamond-shaped halfband digital filters suitable for sampling structure conversion. This formula is accompanied by a multiplierless array structure consisting of two types of modules. However, it is not clear whether one can obtain 2-D digital filters with other shapes of magnitude response in a multiplierless manner using this method. Furthermore, array realization of the resulting transfer function using De Casteljau algorithm, as shown in [17], does not result in a structure with identical modules of the same type. Specifically, two types of modules are needed, each requiring one type of delay element.

The approach we adopt in this paper relies on the 1-D De Casteljau algorithm and Bernstein representation as its backbone. The most distinguished feature of this approach is that one and only one type of module is needed with two types of delay elements for each module. Furthermore, connection of the modules is very similar to that of the array structure for 1-D filters. Consequently, the transfer function of the resulting array can be analyzed based on existing 1-D results. In fact the proposed method can be viewed as an approach per-

Manuscript received July 17, 1996.

Manuscript revised November 29, 1996.

[†]The author is with the Department of Electrical Engineering, K.N.T. University of Technology, Tehran, Iran.

^{††}The author is with the Center for Research and Development of Educational Technology, Tokyo Institute of Technology, Tokyo, 152 Japan.

^{†††}The author is with the Faculty of Engineering, Tokyo Institute of Technology, Tokyo, 152 Japan.

taining to the same category as McClellan transform designs. For a McClellan transform, there exists an associated Chebyshev structure [9] that is able to realize various 2-D digital filters by appropriate adoption of tap coefficients and a single transformation function. In the case of the proposed array, we have an array structure with fixed boundary coefficients that can be realized in a multiplierless manner, and two types of transformation functions that should be selected according to the desired magnitude response shape. We should also pay additional attention to the two transformation functions and make sure that their multiplierless realization is possible. We will show that it is possible to generate various magnitude response shapes and analyze their characteristics in a simple manner. Compared to the McClellan transform designs, which require different tap coefficients for different filter orders, the proposed arrays are not only multiplierless but can also be modified to higher or lower orders very regularly and without any need to specify additional multiplier coefficients or making change to the consisting modules. For existing approaches to multiplierless design of 2-D FIR filters see for example [23].

We will not analyze the tolerance of the filter to destruction of one or more modules in this paper, but it is expected that the robust performance has been inherited from the 1-D arrays. Actual VLSI implementation of the resulting filter using the proposed array, is a decision that should be arrived at considering various tradeoffs in terms of modularity, lack of multiplier coefficients, simple order modification, high throughput and robust performance with respect to module destruction as merits and large number of delay elements and adders, as a drawback. One can also view this approach as a quick method for transfer function design and merely utilize its strength in design of 2-D and higher dimensional digital filters.

This paper consists of 6 Sections. In Sect.2 we briefly review 1-D array structures proposed for linear phase multiplierless FIR digital filters. In the following Section, general array structures for 2-D linear phase FIR digital filters are proposed and their fundamental properties are analyzed. Section 4 presents a few design examples and guidelines. This is followed by a discussion about multiplierless design, complexity and programmability of the array in Sect.5. Finally, the paper is concluded in Sect.6.

2. Review of Multiplierless Array Structures for 1-D Linear Phase FIR Digital Filters

In this section, we briefly review the 1-D version of the array structures of concern in this paper and mention some of their fundamental properties. The array structures proposed in [10],[13] and [16] may be defined as time-domain realizations of the generalized frequency

domain recurrence

$$H_{i,j}(\omega) = F(\omega)H_{i,j-1}(\omega) + G(\omega)H_{i-1,j}(\omega) + (1 - F(\omega) - G(\omega))H_{i-1,j-1}(\omega) \quad (1)$$

where,

$$\begin{aligned} F(\omega) &= f_0 + f_1 \cos(\omega) \\ G(\omega) &= g_0 + g_1 \cos(\omega) \end{aligned} \quad (2)$$

and real coefficients f and g are chosen appropriately for each filter. This general recurrence needs a set of boundary conditions that are assumed to be as

$$\begin{cases} H_{i,0}(\omega) = p & \dots & i > 0 \\ H_{0,j}(\omega) = q & \dots & j > 0 \\ H_{0,0}(\omega) = r \end{cases} \quad (3)$$

where p, q and r are real numbers called “boundary (multiplier) coefficients.” Figure 1 (b) depicts the array realization of the recurrence. In this array, all modules or Processing Elements (PEs) are identical and realize the 1-D 3-input-1-output FIR system defined by (1) in the time domain. It can be easily verified that the resulting filter at the output of the i -th row and the j -th column of the array, i.e., $H_{i,j}(\omega)$, is a type 1, linear phase 1-D FIR digital filter. If the PEs are realized in a causal manner with the minimum required amount of delay, the resulting filter is of order $2(i + j - 1)$ at most. One should not get confused with the schematic representation of the PEs in Fig. 1 (b); these are 3-input-1-output systems and all three outputs are exactly the same. We shall call the filters $F(\omega)$ and $G(\omega)$ “kernel filters” or simply “kernels.” Figure 1 (a) illustrates the interconnection of the kernels. At this stage of development, there are simple properties that hold for arbitrary choices of the coefficients f and g . We will list these properties below.

Property 1: The frequency response of an array with boundary coefficients $p = q = r = 1$ is identically unity. In other words, the filter degenerates to a trivial allpass system.

Comments: This Property is a simple consequence of the fact that the frequency responses of the three 1-D kernel filters that operate on the three inputs of each module add up to unity. For a rigorous proof, apply an induction on i and j .

Property 2: Denoting by $\bar{H}_{i,j}(\omega)$ the frequency response of an array with boundary conditions,

$$\begin{cases} H_{i,0}(\omega) = 1 - p & \dots & i > 0 \\ H_{0,j}(\omega) = 1 - q & \dots & j > 0 \\ H_{0,0}(\omega) = 1 - r \end{cases} \quad (4)$$

and the same kernel filters as (2), the following relationship holds:

$$\bar{H}_{i,j}(\omega) = 1 - H_{i,j}(\omega) \quad (5)$$

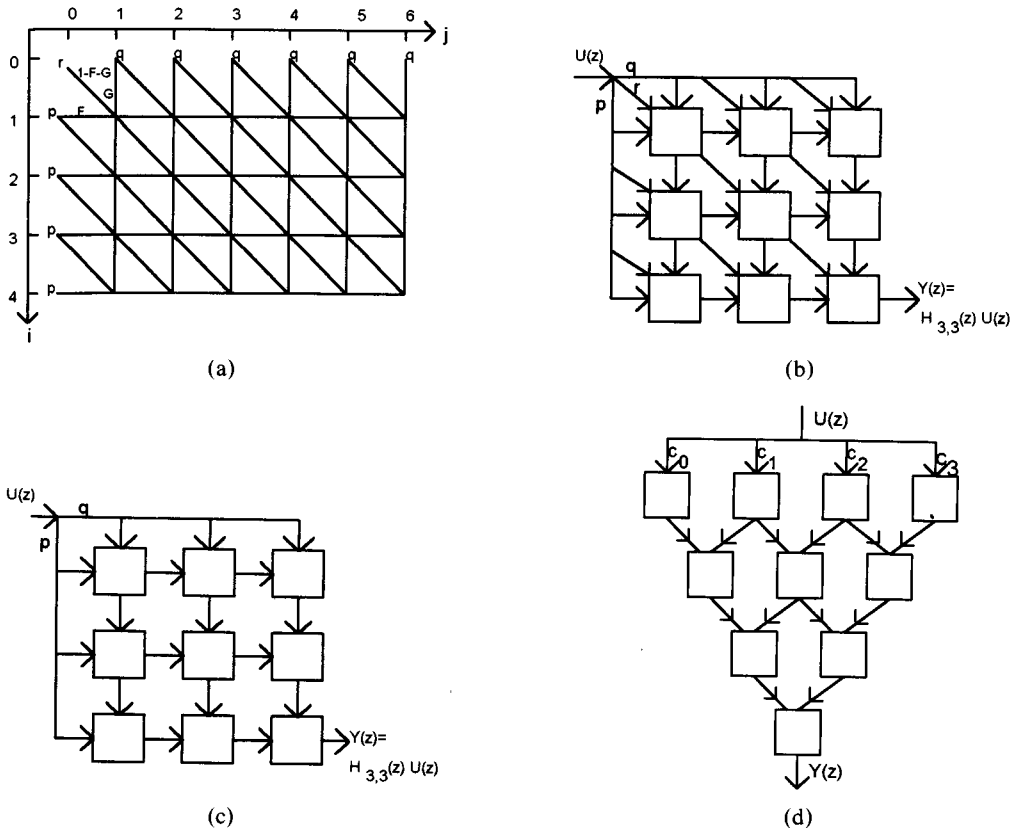


Fig. 1 (a) Schematic representation of interconnection of kernel filters; (b) array realization of recurrence (1) for $i = j = 3$; (c) simplified array under the condition $F(\omega) + G(\omega) = 1$; (d) triangular interconnection of modules for a De Castelju filter.

Table 1 Some kernels and boundary multipliers yielding 1-D frequency selective magnitude responses for a $L \times K$ array.

$F(\omega)$	$\frac{1 + \cos(\omega)}{2}$	$\frac{1 + \cos(\omega)}{2}$	$\frac{1 + (2q - 1) \cos(\omega)}{2q}$
$G(\omega)$	$\frac{1 - \cos(\omega)}{2}$	$\frac{1 - \cos(\omega)}{2}$	$\frac{1 - (2q - 1) \cos(\omega)}{2q}$
$1 - F(\omega) - G(\omega)$	0	0	$(q - 1)/q$
p	1	p	1
q	0	q	0
r	0	0	0
Filter Type	Lowpass Maximally Flat	General form Maximally Flat	Lowpass Non-Maximally Flat
Remarks	$H(0) = 1$ $H(\pi) = 1$ $\left. \frac{\partial^r H}{\partial \omega^r} \right _{\omega=0} = 0, r = 1, \dots, 2L - 1$ $\left. \frac{\partial^r H}{\partial \omega^r} \right _{\omega=\pi} = 0, r = 1, \dots, 2K - 1$ cf. [10], [13]	$H(0) = p$ $H(\pi) = q$ $\left. \frac{\partial^r H}{\partial \omega^r} \right _{\omega=0} = 0, r = 1, \dots, 2L - 1$ $\left. \frac{\partial^r H}{\partial \omega^r} \right _{\omega=\pi} = 0, r = 1, \dots, 2K - 1$ cf. [13]-[15]	Ripples may exist. $1 \leq q \leq 2$ cf. [16]

Comments: Property 2, is a simple consequence of Property 1 and the fact that the frequency response is linear with respect to the boundary coefficients. In fact, (5) can be viewed as a transformation operating on the

boundary coefficients that yields a complementary filter pair. Other useful properties will be presented as Theorems for the general 2-D case later in Sect. 3.

Next we consider a special case of recurrence (1)

by letting $F(\omega) + G(\omega) = 1$. Under this assumption, the associated array structure can be simplified as shown in Fig. 1(c). Evidently, the diagonal multiplier coefficient r is irrelevant for this structure and the PEs operate as double-input-single-output systems, characterized by coefficients f_i . This array structure is a pruned form of the De Casteljau filter. For further information on the De Casteljau algorithm and corresponding digital filter structures see [22] and [13]. Here, we suffice it to mention that the De Casteljau algorithm evaluates a polynomial expressed in the Bernstein form [21] through a triangular structure [22]. However, for polynomial evaluation tasks, each PE multiplies $1 - x$ and x by its two input signals and then adds up the result, instead of operating as a 2-input-1-output digital filter with kernels $F(\omega)$ and $G(\omega) = 1 - F(\omega)$. In fact, the De Casteljau filters may be obtained by transforming the polynomial variable x into a linear function of $\cos(\omega)$. Some interesting and meaningful choices for the boundary coefficients and the kernel filters are given in Table 1. For detailed discussions and examples see corresponding references. All filters listed in the Table share the important feature that modification of filter order for narrowing or widening of transition band-width does not require any change in kernels or boundary coefficients, and can be achieved by adding or deleting extra rows and/or columns.

3. Array Structures for 2-D Linear Phase FIR Digital Filters and Their Fundamental Properties

The 1-D filters reviewed in the preceding section can be extended to 2-D filters by direct application of the McClellan transform to the kernel filters (2). For a transformation function of the form

$$\begin{aligned} \cos \omega \leftarrow & a_0 + a_1 \cos \omega_1 + a_2 \cos \omega_2 \\ & + a_3 \cos(\omega_1 + \omega_2) + a_4 \cos(\omega_1 - \omega_2) \end{aligned}$$

the kernels of the resulting filter may be written as

$$\begin{aligned} F(\omega_1, \omega_2) &= s_0 + s_1 \cos \omega_1 + s_2 \cos \omega_2 \\ &+ s_3 \cos(\omega_1 + \omega_2) + s_4 \cos(\omega_1 - \omega_2) \\ G(\omega_1, \omega_2) &= t_0 + c(s_1 \cos \omega_1 + s_2 \cos \omega_2 \\ &+ s_3 \cos(\omega_1 + \omega_2) + s_4 \cos(\omega_1 - \omega_2)) \end{aligned}$$

The above representation can be confirmed by inspecting the relation between the coefficients of the two transformed kernels. In this case one may obtain multiplierless filters by judicious selection of the transformation function and the 1-D kernel coefficients. Although this may yield desirable filters for some cases, the nature of the McClellan transform restricts the coefficients of the transformed kernel as shown in the above equations. As a result, the transformed kernels can enjoy only 7 independent coefficients. In this section we present an extension which provides us with 10 degrees

of freedom in selection of the kernel filters through 10 independent multiplier coefficients that are not necessarily related in the same way as the coefficients of the McClellan transformed kernels. This can lead us to a broader family of 2-D arrays, with various shapes of frequency responses and multiplierless kernels, that contains the family of McClellan-transformed 1-D arrays as a special case. The proposed generalization is as the following.

Consider the general array of Sect. 2 and let the consisting modules be 3-input-1-output 2-D (instead of 1-D) digital systems. In this case, a 2-D linear phase FIR kernel filter operates on each input of the modules and the resulting frequency response at the output of the module (i, j) , i.e., the module located at the i -th row and the j -th column of the array, becomes

$$\begin{aligned} H_{i,j}(\omega_1, \omega_2) &= F(\omega_1, \omega_2)H_{i,j-1}(\omega_1, \omega_2) \\ &+ G(\omega_1, \omega_2)H_{i-1,j}(\omega_1, \omega_2) \\ &+ (1 - F(\omega_1, \omega_2) - G(\omega_1, \omega_2)) \\ &\times H_{i-1,j-1}(\omega_1, \omega_2) \end{aligned} \quad (6)$$

where

$$\begin{aligned} F(\omega_1, \omega_2) &= f_0 + f_1 \cos(\omega_1) + f_2 \cos(\omega_2) \\ &+ f_3 \cos(\omega_1 + \omega_2) + f_4 \cos(\omega_1 - \omega_2) \\ G(\omega_1, \omega_2) &= g_0 + g_1 \cos(\omega_1) + g_2 \cos(\omega_2) \\ &+ g_3 \cos(\omega_1 + \omega_2) + g_4 \cos(\omega_1 - \omega_2) \end{aligned} \quad (7)$$

and f and g are real numbers. In this paper, the boundary conditions are assumed to be

$$\begin{cases} H_{i,0}(\omega_1, \omega_2) = p = 1 & \dots & i > 0 \\ H_{0,j}(\omega_1, \omega_2) = q = 0 & \dots & j > 0 \\ H_{0,0}(\omega_1, \omega_2) = r = 1/2 \end{cases} \quad (8)$$

If the PEs are realized in a causal manner with the minimum required amount of delay, the resulting filter is of order $2(i + j - 1) \times 2(i + j - 1)$ at most. The usefulness of this particular selection will become clear later in this section when we investigate various properties of the array. Note that Properties 1 and 2, given earlier in Sect. 2, hold for the 2-D case as well. In the following, we present Theorems explaining some important properties of (6) under boundary conditions (8). These can be utilized for analyzing the overall frequency response by simple inspection of the kernels. Furthermore, in the next section, we will propose an approach for designing 2-D filters based on solving systems of linear equations formed to satisfy the necessary and sufficient conditions given in these Theorems.

Theorem 1: The necessary and sufficient condition for $H_{i,j}(\omega_1, \omega_2)$ to satisfy $H_{i,j}(\omega_1, \omega_2) = 1$ for arbitrary i and j at angular frequencies ω_1 and ω_2 is that $G(\omega_1, \omega_2) = 0$ and $F(\omega_1, \omega_2) = 1$ hold at these frequencies.

Proof: Sufficiency can be proved by an induction on i and j . Necessity can be proved by writing down equations for the cases $i = j = 1$ and $i = 1, j = 2$ and solving the resulting system for $F(\omega_1, \omega_2)$ and $G(\omega_1, \omega_2)$.

Theorem 2: The necessary and sufficient condition for $H_{i,j}(\omega_1, \omega_2)$ to satisfy $H_{i,j}(\omega_1, \omega_2) = 0$ for arbitrary i and j at angular frequencies ω_1 and ω_2 is that $F(\omega_1, \omega_2) = 0$ and $G(\omega_1, \omega_2) = 1$ hold at these frequencies.

Proof: The proof is similar to that of Theorem 1.

Theorem 3: The necessary and sufficient condition for $H_{i,i}(\omega_1, \omega_2)$ to satisfy $H_{i,i}(\omega_1, \omega_2) = 1/2$ for arbitrary i at angular frequencies ω_1 and ω_2 is that $F(\omega_1, \omega_2) = G(\omega_1, \omega_2)$ holds at these frequencies.

Proof: Sufficiency can be proved by noting that, due to boundary conditions (8) and Property 2, in an array with equal number of modules in horizontal and vertical directions, i.e., $i = j$, replacing $F(\omega_1, \omega_2)$ with $G(\omega_1, \omega_2)$ results in a frequency response of the form $1 - H_{i,i}(\omega_1, \omega_2)$. Now, if $F(\omega_1, \omega_2) = G(\omega_1, \omega_2)$ holds at angular frequencies ω_1 and ω_2 , the array remains unchanged and this new structure would have the same frequency response at these frequencies. This can be written as $H_{i,i}(\omega_1, \omega_2) = 1 - H_{i,i}(\omega_1, \omega_2)$ yielding the sufficient condition. Necessity can be proved by forming an equation for the case of $i = 1$ and solving for $F(\omega_1, \omega_2)$.

Note that the assumptions indicated in Theorems 1, 2 and 3 may be satisfied at a single point or a set of points. Next, we shall consider the flatness of the resulting frequency response characteristics at angle θ with respect to the ω_1 axis, i.e., over a set of points $\{(\omega_1, \omega_2)\}$ of the form

$$\lambda_\theta : \begin{cases} \omega_1 = \omega \cos(\theta) \\ \omega_2 = \omega \sin(\theta) \end{cases} \quad (9)$$

Three special cases will be considered and the results will be given as sufficient conditions in the following Theorems.

Theorem 4: If $F(\omega_1, \omega_2) + G(\omega_1, \omega_2) = 1$ and $F(\omega_1, \omega_2)$ varies over $[0,1]$ for all real values of $\omega \in [-\bar{\omega}, \bar{\omega}]$ for

which the line λ_θ is confined to the region $[-\pi, \pi] \times [-\pi, \pi]$, the resulting frequency response would be maximally flat over λ_θ at the frequencies where $F(\omega_1, \omega_2) = 0$ or $F(\omega_1, \omega_2) = 1$.

Proof: It can be seen that under the indicated condition, all diagonal connections of the filter become zero and may be neglected. Hence the frequency response of the structure at direction θ would be equivalent to that of a 1-D filter as shown in Fig. 2. The diagonal boundary multiplier shown in the figure will not affect the frequency response in this case and the resulting array is a 1-D maximally flat filter [10], [13]. Considering that $F(\omega_1, \omega_2)$ varies over $[0,1]$, the frequency response becomes maximally flat, over the line λ_θ , at the point where $F(\omega_1, \omega_2) = 1$, with degree of flatness determined by i , and at the point where $F(\omega_1, \omega_2) = 0$, with degree of flatness determined by j , and attains the values 1 and 0 at these points, respectively.

Example 1: Consider the following choices for $F(\omega_1, \omega_2)$ and $G(\omega_1, \omega_2)$:

$$\begin{aligned} F(\omega_1, \omega_2) &= 1/2 + 1/2 \cos(\omega_1) \\ G(\omega_1, \omega_2) &= 1/2 - 1/2 \cos(\omega_2) \end{aligned} \quad (10)$$

It is clear that $F(\omega_1, \omega_2) + G(\omega_1, \omega_2) = 1$ over $\lambda_{\pi/4}$, viz. $\omega_1 = \omega_2$, and $F(\omega_1, \omega_2)$ varies from 1 to 0 when $\omega_1 = \omega_2$ varies from 0 to π . According to Theorem 4, $H_{i,j}(\omega_1, \omega_2)$ is maximally flat over the line $\omega_1 = \omega_2$

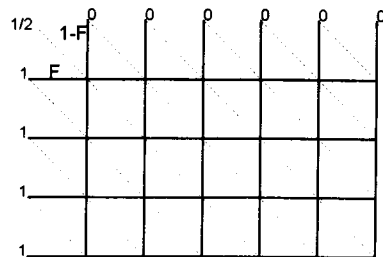
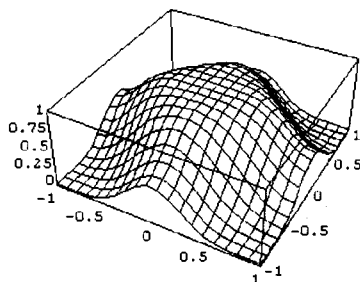
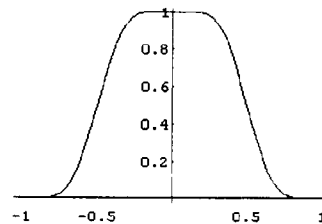


Fig. 2 Connection of kernel filters when the assumption of Theorem 4 holds; $F = F(\omega \cos \theta, \omega \sin \theta)$ and inactive kernels are specified by dotted lines.



(a)



(b)

Fig. 3 Magnitude responses of (a) a 3×3 array; (b) its cross-section over $\omega_1 = \omega_2$ with kernels defined in Example 1 and horizontal axes representing the corresponding normalized radian frequencies.

at $\omega_1 = \omega_2 = 0$ and $\omega_1 = \omega_2 = \pi$ with degrees of flatness determined by i and j , respectively. Figure 3 shows the plot of $H_{3,3}(\omega_1, \omega_2)$ and its cross-section over $\lambda_{\frac{\pi}{4}}$. Increasing the number of rows and columns, one can obtain sharper transition characteristics. It can be seen that this choice of kernels results in a diamond-shaped filter. This filter finds application in sampling structure conversion [17].

Theorem 5: If $F(\omega_1, \omega_2) = 0$ and $G(\omega_1, \omega_2)$ varies over $[0,1]$ for all real values of $\omega \in [-\bar{\omega}, \bar{\omega}]$ for which the line λ_{θ} is confined to the region $[-\pi, \pi] \times [-\pi, \pi]$, the resulting frequency response would be flat or maximally flat over λ_{θ} at the points where $G(\omega_1, \omega_2) = 1$ or $G(\omega_1, \omega_2) = 0$.

Proof: The horizontal connections of the structure may be neglected for the frequencies where $F(\omega_1, \omega_2) = 0$, i.e., frequencies lying over λ_{θ} , and are distinguished with dotted lines in Fig. 4(a). Depending on the relative size of i and j , one of the following three cases may occur.

1) $i > j$

The frequency response is equivalent to that of a “flat” 1-D filter attaining unity where $G(\omega_1, \omega_2) = 0$, with degree of flatness determined by $i - j$, and zero where $G(\omega_1, \omega_2) = 1$, with degree of flatness

determined by j , as shown in Fig. 4(b). Note that the response would not be “maximally flat” because of the existence of a boundary multiplier coefficient equal to $1/2$.

2) $i = j$

The frequency response is equivalent to that of a maximally flat 1-D filter attaining $1/2$ where $G(\omega_1, \omega_2) = 0$ and zero where $G(\omega_1, \omega_2) = 1$, with degree of flatness determined by i , as shown in Fig. 4(c). In other words, it is only possible to enhance the flatness, at the frequency where the response attains zero, by increasing i .

3) $i < j$

The frequency response is identically zero according to Fig. 4(d).

Example 2: For the filter presented in Example 1, we can readily verify that $F(\omega_1, \omega_2) = 0$ over $\omega_1 = \pi$. Although this does not belong to λ_{θ} family of lines, Theorem 5 can be applied to this case with no reservation. It is clear that $G(\pi, \omega_2)$ varies from 0 to 1 when ω_2 varies from 0 to π . According to Theorem 5, $H_{i,i}(\omega_1, \omega_2)$ is maximally flat over the line $\omega_1 = \pi$ at $\omega_2 = 0$ and $\omega_2 = \pi$ with degree of flatness determined by i . Fig-

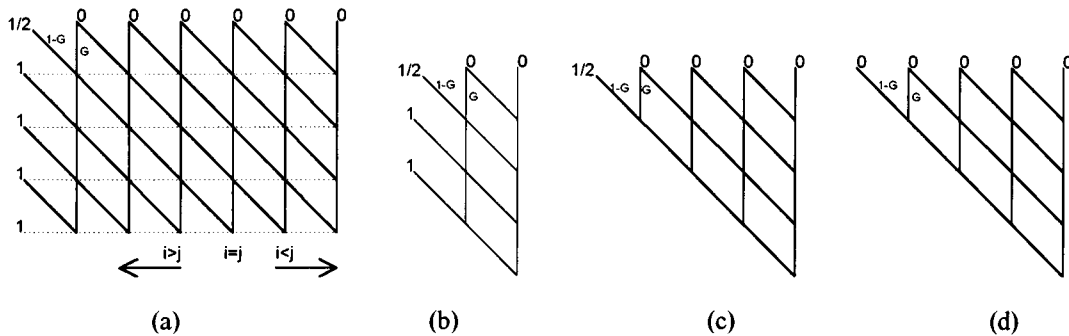


Fig. 4 Connection of kernel filters contributing to the overall frequency response when the assumption of Theorem 5 holds. ($G = G(\omega \cos \theta, \omega \sin \theta)$). (a) Overall connection with inactive kernels specified by dotted lines; (b) connection for $i > j$; (c) connection for $i = j$; (d) connection for $i < j$.

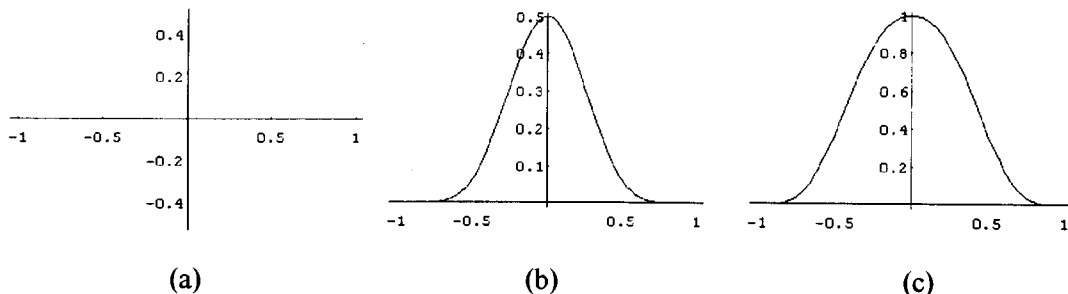


Fig. 5 Cross-sections of magnitude responses of (a) a 2×3 array; (b) a 3×3 array; (c) a 3×2 array with kernels defined in Example 2, over $\omega_1 = \pi$. The horizontal axis represents the normalized radian frequency $\frac{\omega}{\pi}$.

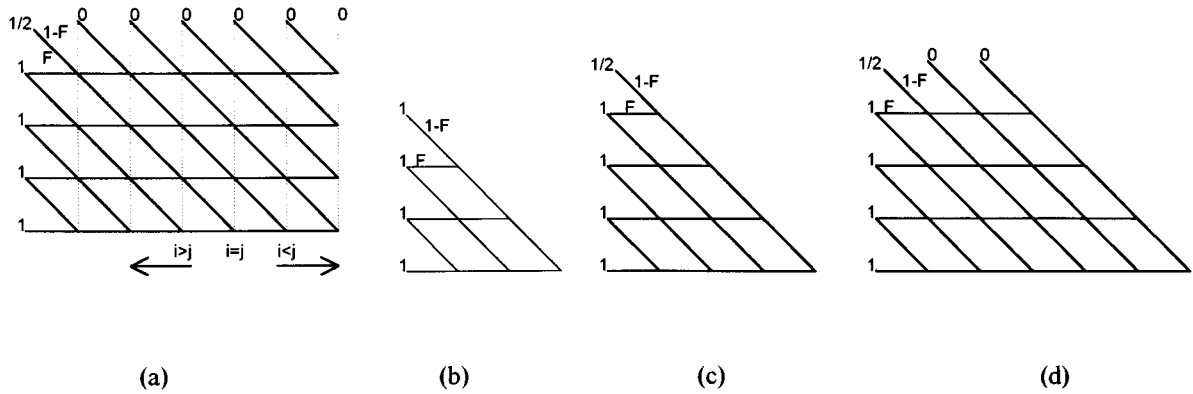


Fig. 6 Connection of kernel filters that contribute to the overall frequency response when the assumption of Theorem 6 holds. (a) Overall connection with inactive kernels shown by dotted lines; (b) connection for $i > j$; (c) connection for $i = j$; (d) connection for $i < j$.

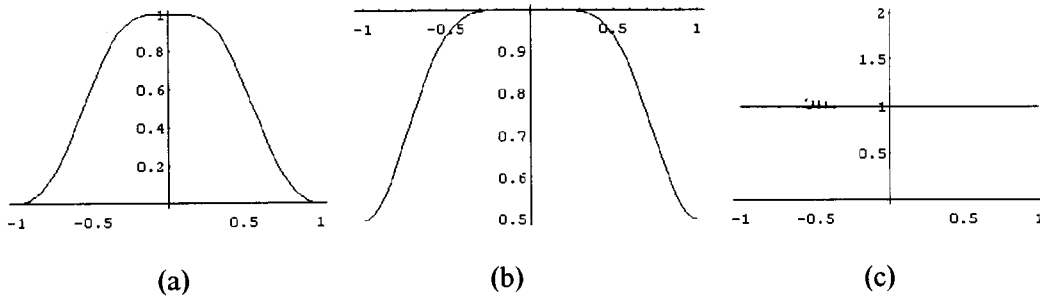


Fig. 7 Magnitude responses of (a) a 2×3 array; (b) a 3×3 array; (c) a 3×2 array with kernels defined in Example 3 over $\omega_2 = 0$. The horizontal axis represents the normalized radian frequency $\frac{\omega}{\pi}$.

ure 5 shows the plots of $H_{2,3}(\omega_1, \omega_2)$, $H_{3,3}(\omega_1, \omega_2)$ and $H_{3,2}(\omega_1, \omega_2)$ over $\omega_1 = \pi$.

Theorem 6: If $G(\omega_1, \omega_2) = 0$ and $F(\omega_1, \omega_2)$ varies over $[0,1]$ for all real values of $\omega \in [-\bar{\omega}, \bar{\omega}]$ for which the line λ_θ is confined to the region $[-\pi, \pi] \times [-\pi, \pi]$, the resulting frequency response is maximally flat over λ_θ at the frequencies where $F(\omega_1, \omega_2) = 1$ or $F(\omega_1, \omega_2) = 0$.

Proof: The vertical connections of the structure may be neglected for the frequencies where $G(\omega_1, \omega_2) = 0$, i.e., frequencies lying over λ_θ , and are distinguished with dotted lines in Fig. 6(a). Depending on the relative size of i and j , one of the following three cases may occur.

1) $i > j$

The frequency response is identically unity according to Fig. 6(b).

2) $i = j$

The frequency response is equivalent to that of a maximally flat 1-D filter attaining 1/2 where $F(\omega_1, \omega_2) = 0$ and unity where $F(\omega_1, \omega_2) = 1$, with degree of flatness determined by i , as shown in Fig. 6(c). In other words, it is only possible to enhance the flatness, at the frequency where the response attains unity, by increasing i .

3) $i < j$

The frequency response is equivalent to that of a “flat” 1-D filter attaining zero where $F(\omega_1, \omega_2) = 0$, with degree of flatness determined by $j - i$, and unity where $F(\omega_1, \omega_2) = 1$, with degree of flatness determined by i , as shown in Fig. 6(d). Note that the response would not be “maximally flat” because of the existence of boundary multiplier coefficient 1/2.

Example 3: For the filter defined in Example 1, it is clear that $G(\omega_1, \omega_2) = 0$ over λ_0 and $F(\omega_1, 0)$ varies from 1 to 0 when ω_1 varies from 0 to π . According to Theorem 6, $H_{i,i}(\omega_1, \omega_2)$, is maximally flat over the line $\omega_2 = 0$ at $\omega_1 = 0$ and $\omega_1 = \pi$ with degree of flatness determined by i . Figure 7 shows the plots of $H_{2,3}(\omega_1, \omega_2)$, $H_{3,3}(\omega_1, \omega_2)$ and $H_{3,2}(\omega_1, \omega_2)$ over λ_0 .

The following Theorem presents a sufficient condition for halfbandness of the filter for the case where there are equal number of PEs in each row and column.

Theorem 7: A sufficient condition to obtain halfband filters at the output of the main diagonal modules at arbitrary locations is that

$$F(\pi - \omega_1, \pi - \omega_2) = G(\omega_1, \omega_2)$$

$$G(\pi - \omega_1, \pi - \omega_2) = F(\omega_1, \omega_2)$$

hold at all frequencies $(\omega_1, \omega_2) \in [-\pi, \pi] \times [-\pi, \pi]$.

Proof: Under this condition, $H_{i,i}(\pi - \omega_1, \pi - \omega_2)$ is equivalent to the frequency response of a filter with $F(\omega_1, \omega_2)$ as the vertical kernel and $G(\omega_1, \omega_2)$ as the horizontal kernel. This is equivalent to changing boundary coefficients as

$$\begin{cases} p \leftarrow 1 - p \\ q \leftarrow 1 - q \\ r \leftarrow 1 - r \end{cases}$$

but due to Property 2 of Sect. 2, the frequency response after such a transformation becomes $1 - H_{i,i}(\omega_1, \omega_2)$ and we get

$$H_{i,i}(\pi - \omega_1, \pi - \omega_2) = 1 - H_{i,i}(\omega_1, \omega_2).$$

This is the definition of a 2-D half-band filter.

4. Design Examples and Guidelines

In this section we consider various examples of linear phase filters with practical applications in 2-D filtering. The Theorems and Properties stated in Sects. 2 and 3 will come in handy for our purpose of determining meaningful values for coefficients f and g of the kernel filters. Our approach is based on solving systems of linear equations.

4.1 Designs Satisfying Constraints at Four Specific Frequencies

The first class of filters we consider here, satisfy simple frequency response constraints at frequencies $\omega_i = 0, \pi$, namely,

$$\begin{cases} H_{i,j}(0, 0) = \frac{1 + (-1)^{p_{00}}}{2} \\ H_{i,j}(0, \pi) = \frac{1 + (-1)^{p_{01}}}{2} \\ H_{i,j}(\pi, 0) = \frac{1 + (-1)^{p_{10}}}{2} \\ H_{i,j}(\pi, \pi) = \frac{1 + (-1)^{p_{11}}}{2} \end{cases} \quad (11)$$

where $i, j, p_{00}, p_{01}, p_{10}, p_{11}$ are positive integers. Evidently, by adopting an even or odd value for p , the right-hand sides of (11) can be forced to become unity or zero, respectively. The above setting can yield all 16 possible combinations of zeros and ones at the specified frequencies. Invoking Theorems 1 and 2, we can form a system of eight linear equations (two equations as constraints over $F(\omega_1, \omega_2)$ and $G(\omega_1, \omega_2)$ for each equation of (11)) with ten unknowns. This can be solved as

$$\begin{aligned} f_0 &= \frac{1}{2} + \frac{(-1)^{p_{00}} + (-1)^{p_{01}} + (-1)^{p_{10}} + (-1)^{p_{11}}}{8} \\ f_1 &= \frac{(-1)^{p_{00}} + (-1)^{p_{01}} - (-1)^{p_{10}} - (-1)^{p_{11}}}{8} \end{aligned}$$

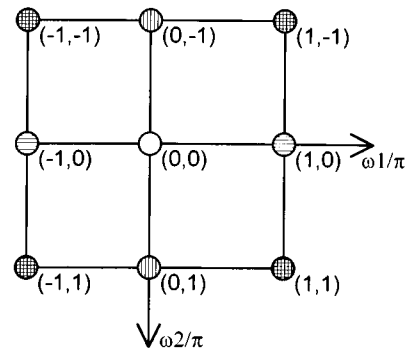


Fig. 8 Nine points at which magnitude response is fixed by kernels defined in (12) and (13); points with the same hashing assume the same magnitude responses.

$$\begin{aligned} f_2 &= \frac{(-1)^{p_{00}} - (-1)^{p_{01}} + (-1)^{p_{10}} - (-1)^{p_{11}}}{8} \\ f_3 &= \frac{(-1)^{p_{00}} - (-1)^{p_{01}} - (-1)^{p_{10}} + (-1)^{p_{11}}}{8} \\ &\quad - f_4 \end{aligned} \quad (12)$$

$$\begin{aligned} g_0 &= \frac{1}{2} - \frac{(-1)^{p_{00}} + (-1)^{p_{01}} + (-1)^{p_{10}} + (-1)^{p_{11}}}{8} \\ g_1 &= \frac{-(-1)^{p_{00}} - (-1)^{p_{01}} + (-1)^{p_{10}} + (-1)^{p_{11}}}{8} \\ g_2 &= \frac{-(-1)^{p_{00}} + (-1)^{p_{01}} - (-1)^{p_{10}} + (-1)^{p_{11}}}{8} \\ g_3 &= \frac{-(-1)^{p_{00}} + (-1)^{p_{01}} + (-1)^{p_{10}} - (-1)^{p_{11}}}{8} \\ &\quad - g_4 \end{aligned} \quad (13)$$

Although the above solution satisfies the given constraints for arbitrary values of i and j , the actual values of f_4 and g_4 , taken as parameters here, remain to be determined. When flatness is of concern, the effect of these two coefficients on the overall frequency response can be examined using Theorems 4, 5 and 6. An interesting consequence of the above setting is that the frequency response gets restricted at 5 other points as shown in Fig. 8. That is,

$$\begin{aligned} H_{i,j}(0, \pi) &= H_{i,j}(0, -\pi) \\ H_{i,j}(\pi, 0) &= H_{i,j}(-\pi, 0) \\ H_{i,j}(\pi, \pi) &= H_{i,j}(-\pi, \pi) \\ &= H_{i,j}(\pi, -\pi) = H_{i,j}(-\pi, -\pi) \end{aligned}$$

A note is in order here on the values of f_4 and g_4 . Considering the fact that $f_1 = -g_1$, and $f_2 = -g_2$, if f_4 and g_4 are chosen such that $f_3 = -g_3$, or equivalently if we take $f_4 = -g_4$, the resulting 2-D filter is nothing but a McClellan transformed 1-D filter defined by the recurrence

$$\begin{aligned} H_{i,j}(\omega) &= (f'_0 + \cos(\omega))H_{i,j-1}(\omega) \\ &\quad + (g'_0 - \cos(\omega))H_{i-1,j}(\omega) \\ &\quad + (1 - f'_0 - g'_0)H_{i-1,j-1}(\omega) \end{aligned} \quad (14)$$

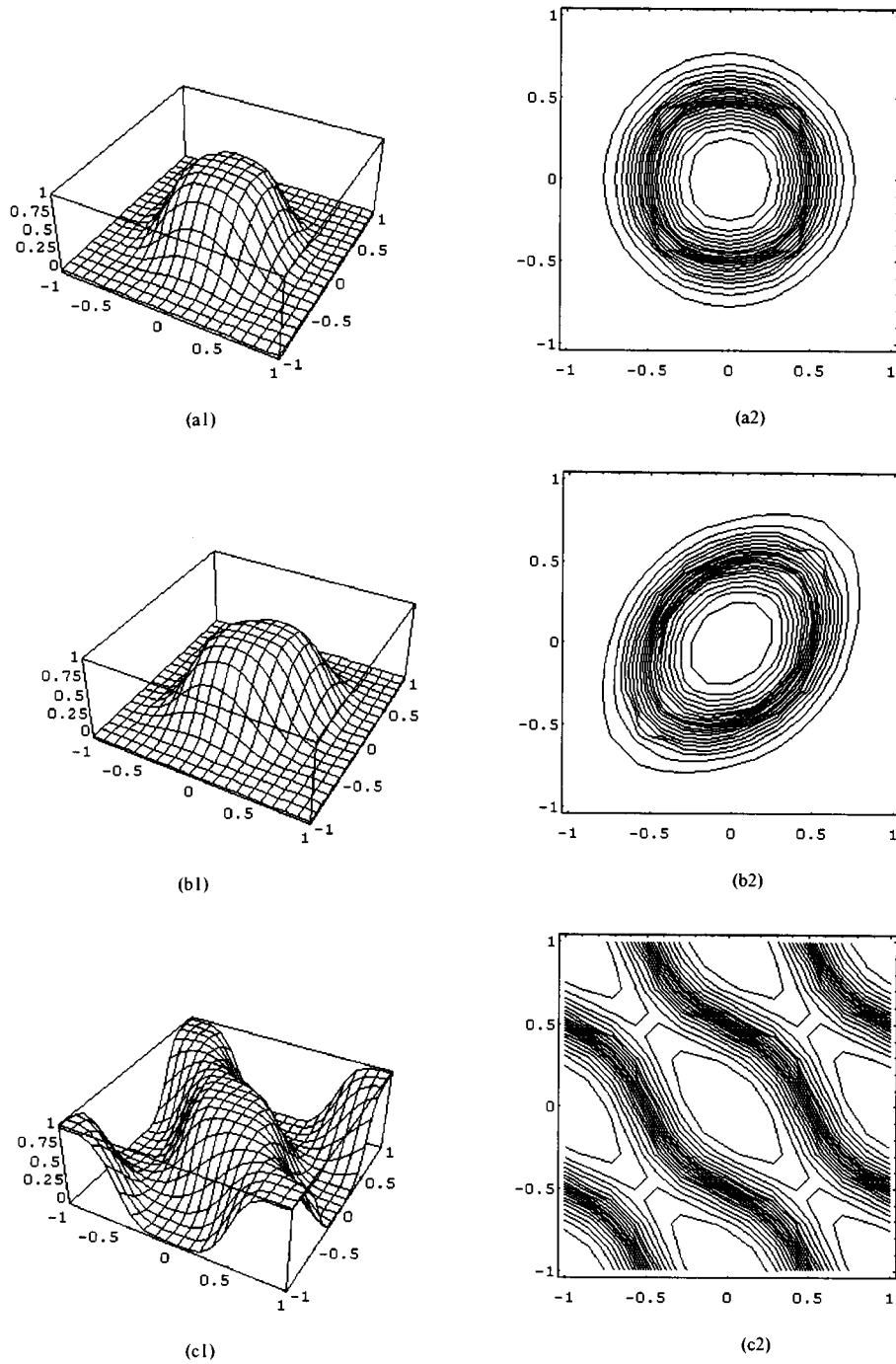


Fig. 9 (a1)–(c2) Examples of magnitude responses (bird-eye view and contour plot) of various 2-D filters realizable with multiplierless 3×3 arrays. The horizontal axes represent the normalized radian frequencies $\frac{\omega_1}{\pi}$ and $\frac{\omega_2}{\pi}$. For kernel coefficients see Table 2.

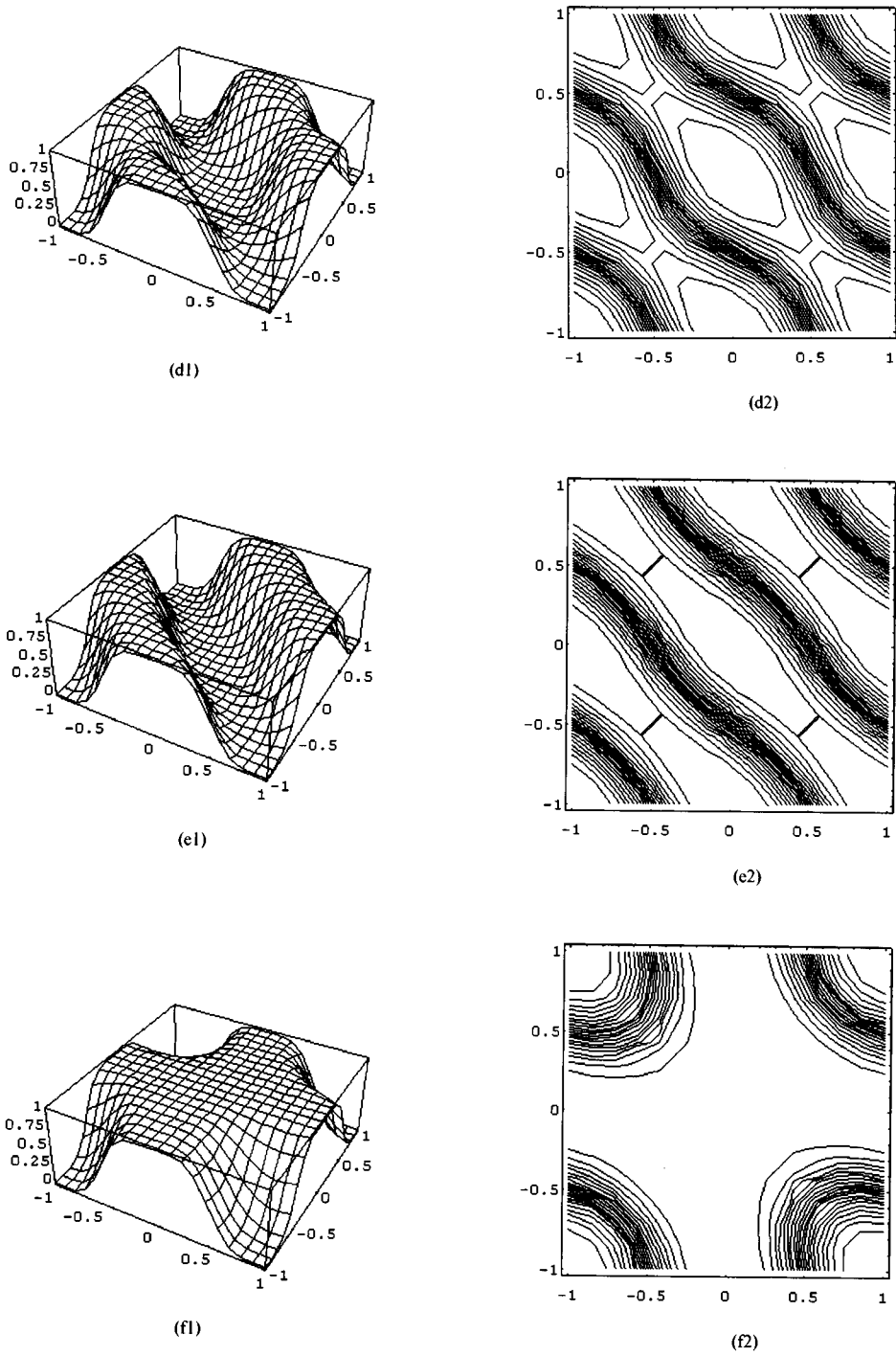
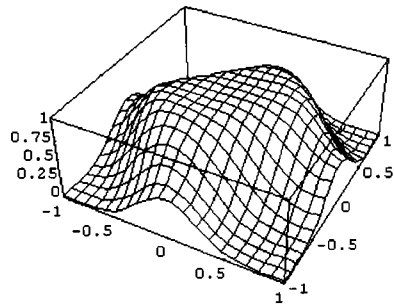
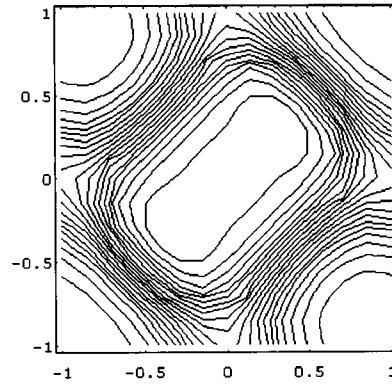


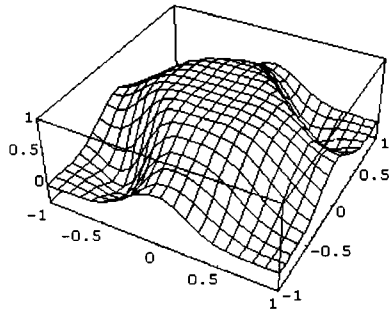
Fig. 9 (d1)-(f2) (Continued)



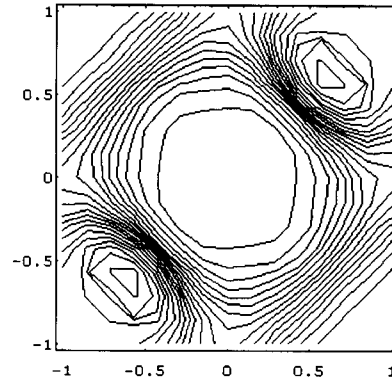
(g1)



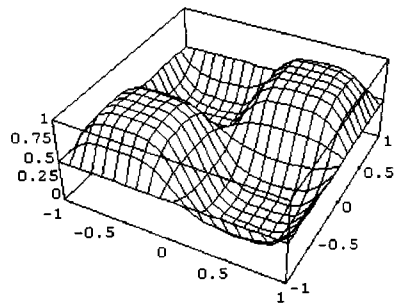
(g2)



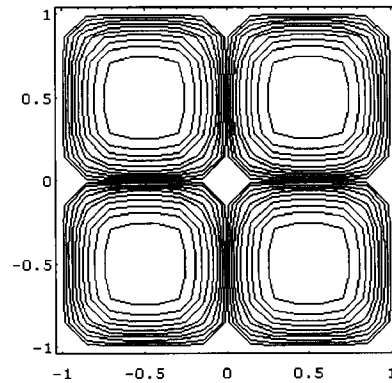
(h1)



(h2)



(i1)



(i2)

Fig. 9 (g1)-(i2) (Continued)

Table 2 Coefficients of kernel filters for arrays with magnitude responses plotted in Fig. 9.

	$\{f_0, f_1, f_2, f_3, f_4\}$	$\{g_0, g_1, g_2, g_3, g_4\}$
(a)	$\left\{\frac{1}{4}, \frac{1}{4}, \frac{1}{4}, 0, \frac{1}{4}\right\}$	$\left\{\frac{3}{4}, \frac{-1}{4}, \frac{-1}{4}, \frac{-1}{4}, 0\right\}$
(b)	$\left\{\frac{1}{4}, \frac{1}{4}, \frac{1}{4}, 0, \frac{1}{4}\right\}$	$\left\{\frac{3}{4}, \frac{-1}{4}, \frac{-1}{4}, \frac{-1}{8}, \frac{7}{8}\right\}$
(c)	$\left\{\frac{1}{2}, 0, 0, \frac{1}{4}, \frac{1}{4}\right\}$	$\left\{\frac{1}{2}, 0, 0, \frac{-1}{2}, 0\right\}$
(d)	$\left\{\frac{1}{2}, 0, 0, \frac{-1}{4}, \frac{-1}{4}\right\}$	$\left\{\frac{1}{2}, 0, 0, \frac{1}{2}, 0\right\}$
(e)	$\left\{\frac{1}{2}, 0, 0, \frac{-3}{8}, \frac{-1}{8}\right\}$	$\left\{\frac{1}{2}, 0, 0, \frac{1}{2}, 0\right\}$
(f)	$\left\{\frac{3}{4}, \frac{1}{4}, \frac{1}{4}, \frac{-1}{8}, \frac{-1}{8}\right\}$	$\left\{\frac{1}{4}, \frac{-1}{4}, \frac{-1}{4}, \frac{1}{4}, 0\right\}$
(g)	$\left\{\frac{3}{4}, \frac{1}{4}, \frac{1}{4}, \frac{-1}{4}, 0\right\}$	$\left\{\frac{3}{4}, \frac{-1}{4}, \frac{-1}{4}, \frac{-1}{8}, \frac{-1}{8}\right\}$
(h)	$\left\{\frac{3}{4}, \frac{1}{4}, \frac{1}{4}, \frac{-1}{4}, 0\right\}$	$\left\{\frac{3}{4}, \frac{-1}{4}, \frac{-1}{4}, \frac{-3}{8}, \frac{1}{8}\right\}$
(i)	$\left\{\frac{1}{2}, 0, 0, \frac{-1}{2}, 0\right\}$	$\left\{\frac{1}{2}, 0, 0, 0, \frac{-1}{2}\right\}$

We prefer to avoid this case and focus our attention on designs that are not related to the McClellan transforms. Figure 9 and Table 2 include some examples of the filters obtained from (12) and (13) together with respective values of f_4 and g_4 .

4.2 Other Examples

As another example, we can consider filters satisfying a set of constraints including those stated in Theorem 3. For example we can consider constraints of the form

$$\begin{cases} H_{i,j}(0, 0) = 1 \\ F(0, \pi) = 1 \\ G(0, \pi) = 1 \\ F(\pi, 0) = 1 \\ G(\pi, 0) = 1 \\ H_{i,j}(\pi, \pi) = 0 \end{cases} \quad (15)$$

which is equivalent to a system of 8 linear equations in 10 unknowns. Two examples of the solution are shown in Figs. 9 (g1), (g2), (h1) and (h2).

As another example, a simple kernel pair of the form

$$\begin{aligned} F(\omega_1, \omega_2) &= \frac{1 - \cos(\omega_1 + \omega_2)}{2} \\ G(\omega_1, \omega_2) &= \frac{1 - \cos(\omega_1 - \omega_2)}{2} \end{aligned} \quad (16)$$

results in a fan filter as shown in Figs. 9 (i1) and (i2). It should be noted that for a 1×1 2-D array, the kernels specified by (16) yield the same filter as the McClellan transform of a 1×1 1-D maximally flat array using

$\cos(\omega) \leftarrow \sin(\omega_1) \sin(\omega_2)$ as given in [1]. However for larger arrays the two yield different filters. Finally, for all above examples the plots are given for arrays of size 3×3 . Evidently, increasing the array size in both directions results in sharper transition band-widths.

5. Multiplierless Realization, Complexity and Programmability

The above-mentioned examples share an important property: kernel filters can be realized free of multipliers using simple bit-shift operations. It is obvious that the entire array can be realized free of multiplier coefficients so long as the kernel filters preserve this property. The examples given in the previous Sections are among the filters that enjoy this property. Moreover, this property has a major effect on simplifying design stage of the filter; we only need to make sure that the kernels are multiplierless and this can be accomplished by controlling only 10 coefficients regardless of the order of the filter or size of the array.

An important point to consider is the complexity of the array in terms of the number of adders and delay elements. The number of adders depend on two matters: (1) number of non-zero kernel coefficients and (2) relationship between the values of different coefficients. The effect of (1) is straight-forward and amounts to a smaller number of adders if more zero-valued coefficients exist. However, (2) has a more complex effect and the reduction depends on the possibility of sharing different computation results. The number of adders for an $L \times K$ array can be expressed as

$$A = c_a LK \quad (17)$$

where L and K denote the number of rows and columns respectively, and c_a being the number of adders at each PE is an integer independent of L and K .

To estimate the required number of delay elements, we should obtain the z-transform of the kernel transfer function. This can be done by setting $\cos(\omega_i) = \frac{z_i + z_i^{-1}}{2}$ and making necessary modifications to render the realization causal. The latter operation results in appearance of delay elements at diagonal connections and horizontal boundary inputs. Vertical boundary inputs receive zero signals and no delays are needed. The total number of delays also depends on whether a systolic realization is of interest or not. For a systolic realization, additional delay elements should be introduced at the outputs of the modules to make independent activity of the modules possible. We can express these effects using

$$M_i = c_{M1i} LK + c_{M2i} (L - 1)K + c_{M3i} (L - 1) \quad (18)$$

where c_{M1i} , c_{M2i} and c_{M3i} denote the number of z_i delay elements used at each module, diagonal connection and horizontal boundary input, respectively. These coefficients are independent of the number of rows and

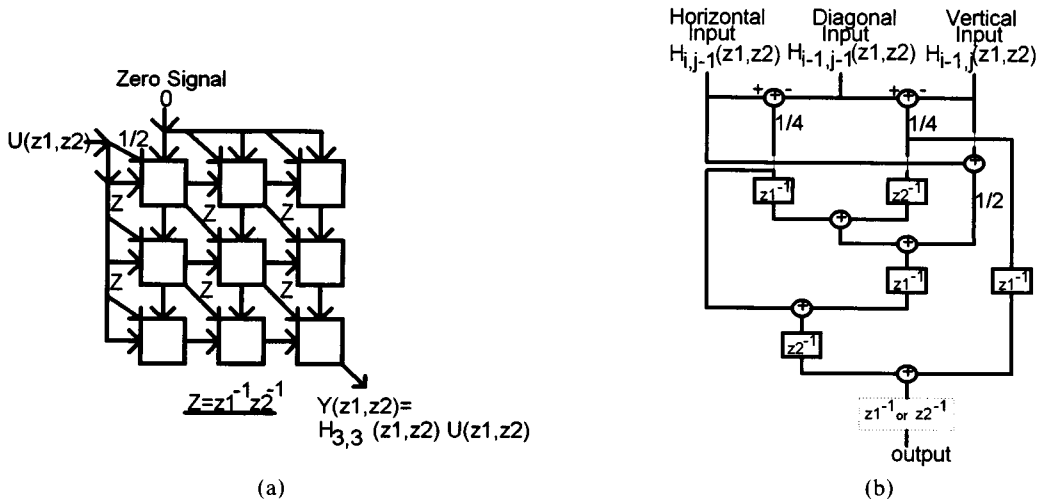


Fig. 10 Block diagram of (a) a 3×3 causal array; (b) a realization of the constituent PEs for the kernels proposed in Examples 1-3, Sect. 3. The dotted delay block may be added for pipelining. When this block is active, the delay elements at diagonal connections and boundary inputs of (a), denoted by Z , should be altered as Zz_1^{-1} or Zz_2^{-1} accordingly.

columns but take on different values for systolic and non-systolic realizations.

As an example of actual module structures for a multiplierless realization we present a causal realization of the modules for the kernel filters discussed in Examples 1-3 in Sect. 3. Figure 10 illustrates module interconnection and realization for a 3×3 causal array. In Fig. 10(a), each PE is assumed to realize the causal digital system

$$\begin{aligned}
 H_{i,j} = & z_2^{-1} \left(\frac{2z_1^{-1} + 1 + z_1^{-2}}{4} \right) H_{i,j-1}^{(0)} \\
 & + z_1^{-1} \left(\frac{2z_2^{-1} - 1 - z_2^{-2}}{4} \right) H_{i-1,j}^{(0)} \\
 & + \left(\frac{z_1^{-1} + z_1^{-1}z_2^{-2} - z_2^{-1} - z_1^{-2}z_2^{-2}}{4} \right) H_{i-1,j-1}^{(0)}
 \end{aligned} \tag{19}$$

and thus appropriate delays have been inserted at diagonal connections and boundary inputs to maintain the timing of data flow. The signal flow graph (SFG) of Fig. 10(b) presents a possible realization of the PEs, requiring 7 adders, three z_1 (row direction) delays, two z_2 (column direction) delays and three bit-shift operations. Note, that no multiplication is needed. An equivalent SFG can be obtained realizing the PEs with two z_1 delays, three z_2 delays and the same number of adders. A systolic array can be obtained by doubling the delays at diagonal connections and boundary inputs, and activating the dotted delay block of the SFG (cf. Fig. 10(b)). In the resulting systolic array, all PEs are active in parallel and the output signals can be obtained at a speed roughly proportional to $2T_a$, the time required for performing the two additions needed in the critical path of

Fig. 10(b).

One can view (6) only as a recurrence for designing 2-D transfer functions and turn into other methods for actual realization. In this case, one possible method, that may be less complex in terms of the number of adders and delay elements and more complex in terms of the number of multiplier coefficients, is based on representing the overall transfer function using kernel filters. For instance, $H_{3,3}(\omega_1, \omega_2)$ can be written as

$$\begin{aligned}
 H_{3,3} = & \frac{1}{2} + \frac{3}{2}(F - G) + \frac{3}{2}(-F^2 + G^2) \\
 & + \frac{1}{2}(F^3 - G^3) + \frac{9}{2}(F^2G - FG^2) \\
 & + 3(-F^3G + FG^3) + 3(F^3G^2 - F^2G^3)
 \end{aligned} \tag{20}$$

where the two frequency variables are removed for sake of simplicity. Note that the above expression is not in its simplest form and there are parts that can be shared between different terms. From this simple example we merely wish to show that the filter can be realized using the two kernels as building blocks plus some multiplier coefficients. These multiplier coefficients are fairly simple for filters of lower orders and get more complex with a wider dynamic range for filters of higher orders.

Another interesting feature of the proposed class of filters is their programmability. To alter the magnitude characteristics, one should simply change the kernel filters appropriately. This has no effect on the array structure (connection of the PEs or boundary conditions), or the coefficients of (20).

6. Conclusion

In this paper we tried to offer a new point of view towards multiplierless and modular design of 2-D FIR linear phase digital filters. We were interested in finding an answer to a simple question: how to connect identical, low-order and simple 2-D systems (also called modules or PEs) in a regular manner to obtain a 2-D digital filter with reasonable magnitude response characteristics. As a desired feature, we also considered whether useful characteristics could be obtained under a very restrictive constraint; the modules should be free of multiplier coefficient. We proposed a general two dimensional array structure as an answer and discussed and analyzed its fundamental properties. We made use of known results and ideas from our previous investigations in 1-D FIR linear phase filters and offered rigorous proofs for our claims expressed as Theorems. Specifically, it was shown that it is possible to make the filter behave as a flat or maximally flat filter over straight lines, restrict the magnitude response to 0, 1/2 or 1 at arbitrary frequencies, or as an obvious extension, over straight lines, or obtain half band filters. To investigate the possibility of obtaining modules free of multiplier coefficients, we offered a few design examples for circular and elliptic lowpass, parallelepiped lowpass and some bandpass and bandstop filters.

Our approach results in a highly modular and regular structure and can be modified to lower or higher orders with simple deletion or addition of consisting modules. Based on what we know about 1-D arrays of the same family, the above-mentioned Theorems on the flatness of the magnitude response over straight lines guarantee that the transition characteristics of the filter becomes sharper for filters of higher order. The array is suitable for special-purpose VLSI realization but needs a large number of adders and memories for filters of high orders. However, in applications such as image processing, higher order filters are usually avoided to prevent ringing effects and the increase in number of adders and delays may be tolerated considering other highly favorable features of the array. If appropriate amount of delay is added to the module outputs, one can localize the dependency of computations within the modules and speed up the processing time needed between adjacent incoming sample to a few addition operations. Furthermore, we expect that the deletion of a faulty module from the array and bypassing the connections over it will only result in a modest deviation from the specified characteristics; a property that has been confirmed for the 1-D maximally flat case [18]. It is even possible to obtain all possible realizations with constant $L + K$ in a very economical way [11].

Although the usefulness of the proposed array was demonstrated through several design examples, it is unknown to what extent this structure is capable of yielding arbitrary shapes of magnitude response. However,

it is clear that a rather wide range of flat filters may be obtained through (12) and (13). Further investigation is also needed towards establishment of a method for optimum selection of the parameters and the number of rows and columns required for given magnitude response specifications. Finally, we note that multidimensional extension of our ideas is straight-forward and the Theorems can be extended readily with simple modifications.

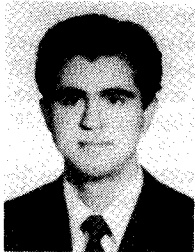
References

- [1] D.E. Dudgeon and R.M. Mersereau, "Multidimensional digital signal processing," Prentice Hall, Inc., Englewoods Cliffs, N.J., 1984.
- [2] T.S. Huang, "Two-dimensional windows," IEEE Trans. Audio Electroacoust., vol.AU-20, no.1, pp.88–89, 1972.
- [3] J.V. Hu and L.R. Rabiner, "Design techniques for two-dimensional digital filters," IEEE Trans. Audio Electroacoust., vol.AU-20, no.4, pp.249–257, 1972.
- [4] Y. Kamp and J.P. Thiran, "Chebyshev approximation for two-dimensional non-recursive digital filters," IEEE Trans. Circuits Syst., vol.CAS-22, no.3, pp.208–218, 1975.
- [5] J.H. Lodge and M.M. Fahmy, "An efficient optimization technique for the design of two-dimensional linear-phase FIR digital filters," IEEE Trans. Acoustics, Speech, and Signal Processing, vol.ASSP-28, no.3, pp.308–313, 1980.
- [6] M.O. Ahmad and J.D. Wang, "An analytic least squares solution to the design problem of two-dimensional FIR filters with quadrantly symmetric or antisymmetric frequency response," IEEE Trans. Circuits Syst., vol.CAS-36, no.7, pp.968–980, 1989.
- [7] J.H. McClellan, "The design of two-dimensional digital filters by transformations," Proc. 7th Annual Princeton Conf. Info. Sci. and Syst., pp.247–251, 1973.
- [8] R.M. Mersereau, W.F.G. Mecklenbraeuker, and T. Quatir Jr., "McClellan transformation for 2-D digital filtering: I-design," IEEE Trans. Circuits Syst., vol.CAS-23, no.7, pp.405–414, July 1976.
- [9] J.H. McClellan and D.S.K. Chan, "A 2-D FIR filter structure derived from the Chebyshev recursion," IEEE Trans. Circuits Syst., vol.CAS-24, no.7, pp.372–378, 1977.
- [10] S. Samadi, T. Cooklev, A. Nishihara, and N. Fujii, "Multiplierless structure for maximally flat linear phase FIR digital filters," Electron. Lett., vol.29, no.2, pp.184–185, 1993.
- [11] T. Cooklev, S. Samadi, A. Nishihara, and N. Fujii, "Efficient implementation of all maximally flat FIR filters of a given order," Electron. Lett., vol.29, no.7, pp.598–599, 1993.
- [12] S. Samadi, A. Nishihara, and N. Fujii, "Stancu operator and FIR digital filters," Proc. 8th Digital Signal Processing Symposium, pp.275–281, 1993.
- [13] S. Samadi, A. Nishihara, and N. Fujii, "Parallel and modular structures for FIR digital filters," IEICE Trans. Fundamentals, vol.E77-A, no.3, pp.467–474, 1994.
- [14] S. Samadi, A. Nishihara, and N. Fujii, "Modular realization of bandstop and bandpass FIR digital filters," 1994 IEEE ISCAS, vol.2, pp.73–76, May 1994.
- [15] S. Samadi, "Design and realization of linear phase digital filters," Ph.D. Dissertation, Tokyo Institute of Technology, 1994.
- [16] S. Samadi, A. Nishihara, and N. Fujii, "Multiplierless arrays for realization of lowpass and highpass linear phase FIR digital filters," IEICE Trans. Fundamentals, vol.E79-A, no.8, pp.1112–1119, Aug. 1996.

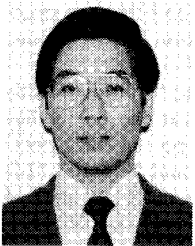
- [17] T. Cooklev, S. Samadi, A. Nishihara, and N. Fujii, "Maximally flat approximation for two-dimensional FIR digital filters with applications in sampling structure conversion," ECCTD'93, Circuit Theory and Design, pp.385-390. Aug. 1993.
- [18] S. Samadi, A. Nishihara, and N. Fujii, "Graceful degradation of maximally flat FIR digital filters," IEICE Trans. Electron., vol.E77-C, no.7, pp.1083-1091, 1994.
- [19] P.J. Davis, "Interpolation and approximation," Dover Publications, Inc. New York, 1975.
- [20] G.G. Lorentz, "Bernstein polynomials," Univ. Toronto Press, Toronto, 1953.
- [21] G.T. Cargo and O. Shisha, "The Bernstein form of a polynomial," Journal of research of the National Bureau of Standards B, vol.70B, no.1, pp.79-81, 1966.
- [22] R.N. Goldman, "Recursive triangles," NATO Adv. Sci. Inst. Ser. C: Math. Phys. Sci., 307, pp.27-71, 1990.
- [23] L. Banzato, N. Benevenuto, and G.M. Cortelazzo, "A design technique for two-dimensional multiplierless FIR filters for video applications," IEEE Trans. Circuits Syst. Video Tech., vol.2, no.3, pp.273-284, Sept. 1992.



Nobuo Fujii received B.E. degree from Keio University, Yokohama, Japan, and M.E. and Doctor of Engineering degrees from Tokyo Institute of Technology, Tokyo, Japan, in 1966, 1968, and 1971, respectively. Since 1971, he has been with the Faculty of Engineering, Tokyo Institute of Technology where he is now a professor in the Department of Physical Electronics. From 1984 to 1985, he was a visiting scholar at the University of California, Santa Barbara. From 1990 to 1992, he served as an editor of the Transaction of the Institute of Electronics, Information, and Communication Engineers and is now one of the chief editors of the International Journal of Analog Integrated Circuits and Signal Processing, Kluwer Academic Publishers. He is the chairman of the technical group of electronic circuits of IEE Japan and the chairman of the Circuits and Systems Society of IEEE Tokyo Chapter. His main interest lies in the fields of active networks, analog integrated circuits, and analog signal processing. He is the recipient of the Best Paper Award of the Institute of Electrical and Communication Engineers of Japan. He is the author of more than 10 books. Dr. Fujii is a member of the Institute of Electrical and Electronics Engineers, and the Institute of Electrical Engineers of Japan.



Saed Samadi was born in Tehran, Iran in 1966. He received the B.E., M.E. and Ph.D. degrees in Physical Electronics from Tokyo Institute of Technology in 1989, 1991 and 1994, respectively. He has been with Khajeh Nassir-Aldin Toosi University of Technology, Tehran, Iran, since 1994. His research interests are in digital signal processing and computational intelligence.



Akinori Nishihara was born in Fukuoka, Japan, on February 26, 1951. He received the B.E., M.E. and Dr.Eng. degrees in electronics from Tokyo Institute of Technology in 1973, 1975 and 1978, respectively. Since 1978 he has been with Tokyo Institute of Technology, where he is now Professor of the Center for Research and Development of Educational Technology. His main research interests are in filter design, 1D and multi-

D signal processing, and modern applications of classical circuit theory. From 1990 to 1994 he served as an Associate Editor of the IEICE Trans. Fundamentals, and is now serving as an Associate Editor of the IEEE Trans. Circuits & Systems II. Dr. Nishihara is a member of IEEE, EURASIP, ECS and JET.